

Published in final edited form as:

Microvasc Res. 2006 November ; 72(3): 161–171. doi:10.1016/j.mvr.2006.05.009.

Secondary lymphedema in the mouse tail: Lymphatic hyperplasia, VEGF-C upregulation, and the protective role of MMP-9

Joseph M. Rutkowski^a, Monica Moya^b, Jimmy Johannes^b, Jeremy Goldman^{b,1}, and Melody A. Swartz^{a,b,*}

^a *Institute of Bioengineering, École Polytechnique Fédérale de Lausanne (EPFL), Lausanne, Switzerland* ^b *Department of Biomedical Engineering, Northwestern University, Evanston, IL, USA*

Abstract

Disturbances in the microcirculation can lead to secondary lymphedema, a common pathological condition that, despite its frequency, still lacks a cure. Lymphedema is clinically well described, but while the genetic underpinnings that cause lymphatic malformations and primary lymphedema are being discovered, the pathophysiology and pathobiology of secondary lymphedema remain poorly understood, partly due to the lack of well-described experimental models. Here, we provide a detailed characterization of secondary lymphedema in the mouse tail and correlate the evolution of tissue swelling to changes in tissue architecture, infiltration of immune cells, deposition of lipids, and proliferation and morphology of the lymphatic vessels. We show that sustained swelling leads to lymphatic hyperplasia and upregulation of vascular endothelial growth factor (VEGF)-C, which may exacerbate the edema because the hyperplastic vessels are poorly functional. The onset of lymphatic hyperplasia occurred prior to the onset of lipid accumulation and peak VEGF-C expression. Langerhans dendritic cells were seen in the dermis migrating from the epidermis to the lymphatic capillaries in edematous tissue. Furthermore, these results were consistent between two different normal mouse strains, but swelling was significantly greater in a matrix metalloproteinase (MMP)-9 null strain. Thus, by characterizing this highly reproducible model of secondary lymphedema, we conclude that VEGF-C upregulation and lymphatic hyperplasia resulting from dermal lymphatic ligation and lymphedema leads to decreased drainage function and that MMP-9 may be important in counteracting tissue swelling.

Keywords

Lymphatic function; Extracellular matrix; Lipid deposition; MMP-9; VEGF-C

Introduction

Lymphedema is a common pathology of tissue fluid balance often due to defects in lymphatic uptake and/or transport. Primary lymphedema results from defects of the lymphatic system leading to insufficiencies in transport, whereas the more common secondary lymphedema arises as a consequence to surgical, malignant, inflammatory, or traumatic disruption of the lymphatics (Rockson, 2001; Witte et al., 2001). As a chronic disease, lymphedema leads to the

*Corresponding author. Laboratory for Mechanobiology and Morphogenesis, Institute of Bioengineering/School of Life Sciences, École Polytechnique Fédérale de Lausanne (EPFL), Station 15, 1015 Lausanne, Switzerland. Fax: +41 21 693 9685. E-mail address: E-mail: melody.swartz@epfl.ch (M.A. Swartz).

¹Current address: Department of Biomedical Engineering, Michigan Technological University, Houghton, MI, USA.

remodeling of skin and subcutaneous tissues (Daroczy, 1995), accumulation of lipids (Schirger et al., 1962), macrophage recruitment (Piller, 1990), and failures in Langerhans dendritic cell migration (Olszewski et al., 1990) in the affected tissue. Unfortunately, this potentially debilitating condition lacks a cure and current treatments for chronic lymphedema, which include regular massage treatments and pressure applications or surgical removal of edematous tissue, can only slow its progression but not reverse the condition (Foldi, 1998; Mortimer, 1997; Witte et al., 2001).

Recent studies have identified key regulators of lymphatic development and the genetic underpinnings of primary lymphedema caused by lymphatic malformation in development. However, the pathophysiology of secondary lymphedema – including the interplay between inflammatory events, matrix remodeling, and local lymphatic response – is less understood, and because of this it is still not clear to what extent therapies aimed at lymphatic regrowth can be used to treat various types of secondary lymphedema. For example, if lymphedema is caused by downstream blockage (e.g., surgical removal of lymph nodes) do the previously healthy lymphatic capillaries respond to the tissue swelling by growing, or by regressing? Do they still facilitate immune cell trafficking? Without an understanding of the tissue lymphatic pathophysiology of secondary lymphedema, rational treatment options will continue to be elusive.

Key molecular players in lymphatic development have been demonstrated primarily by transgenic models; mutations in these regulators commonly lead to either embryonic mortality or lymphatic irregularities and symptoms of primary edema (Oliver and Alitalo, 2005). Prox1, for example, governs the commitment of endothelial cells to a lymphatic lineage in development and Prox1 null embryonic mice die before birth (Wigle and Oliver, 1999), whereas surviving Prox1 heterozygotes possess discontinuous lymphatic endothelium and exhibit abnormal fluid and lipid accumulation in the interstitium (Harvey et al., 2005). Mice lacking angiopoietin-2, thought to play a role in vascular remodeling and lymphatic patterning, have disorganized, irregular lymphatic vessels and exhibit dermal edema and chylous ascites (Gale et al., 2002). Mutations in Foxc2, a transcription factor expressed on developing lymphatics, have been identified as the cause of lymphedema–distichiasis in humans that, unlike other types of congenital lymphedema, is characterized by hyperplastic lymphatic vessels (Brice et al., 2002; Dagenais et al., 2004). Foxc2-null and -heterozygous mice possess hyperplastic lymphatic vessels and malfunctioning lymphatic valves that result in lymphatic backflow and abnormal lymphatic drainage (Kriederman et al., 2003; Petrova et al., 2004). A mutant allele for vascular endothelial growth factor (VEGF) receptor-3 (VEGFR-3) is responsible for Milroy's disease in humans, a congenital disorder characterized by primary lymphedema in the extremities, as well as the Chy mouse phenotype that exhibits lymphatic defects similar to the human condition (Karkkainen et al., 2001). VEGFR-3 and its ligand VEGF-C are also critical for both embryonic (Kukk et al., 1996) and adult lymphangiogenesis (Oh et al., 1997; Pytowski et al., 2005). These findings suggest that targeting lymphatic molecular mechanisms for improving lymphatic function may lead to a successful treatment of lymphedema, and as a result, research has focused on the most well-studied lymphatic molecular pathway to potentially treat conditions of both primary and secondary lymphedema: VEGFR-3 and VEGF-C (Karkkainen et al., 2001; Szuba et al., 2002; Yoon et al., 2003). However, VEGF-C overexpressing mice display hyperplastic lymphatics (Jeltsch et al., 1997) and we recently showed that excess VEGF-C delivered to otherwise normally regenerating skin led to hyperplastic lymphatic vessels without any increase in function (Goldman et al., 2005). The proper resolution of lymphedema is likely dependent on the initial cause of the pathology, and effective treatments for primary and secondary lymphedema are therefore likely to differ. Although the causes of primary lymphedema are increasingly appreciated, there remain gaps in our understanding of the pathophysiology and pathobiology

of secondary lymphedema. These gaps are largely due to the absence of well-characterized models of secondary lymphedema.

Existing models of secondary lymphedema in the dog hindlimb (Han et al., 1985; Olszewski, 1973), rat hindlimb (Kanter et al., 1990; Wang and Zhong, 1985), or rabbit ear (Szuba et al., 2002) disrupt lymphatic transport through the excision of a circumferential band of skin and subcutaneous tissue. These models can sustain significant lymphedema for 3–4 weeks and result in a chronic increase in limb or ear volume. We earlier described a model of secondary lymphedema in the mouse tail skin (Slavin et al., 1999; Swartz et al., 1999). Here, we characterize this model of secondary lymphedema to not only determine the reproducibility across several strains of mice, but moreover, to also describe the relative timing of the appearance of chronic symptoms, such as changes in extracellular matrix structure, accumulation of lipids, and recruitment of macrophages with the overall degree of swelling of the tail skin. We then correlate the timing of the lymphatic response and expression of VEGF-C to these pathological outcomes and show that sustained tissue swelling leads to hyperplasia and subsequent decrease in function of the lymphatic capillaries, closely followed by a drastic increase in local VEGF-C expression. Additionally, to ascertain the importance of matrix metalloproteinases (MMPs) in the inevitable matrix changes during tail swelling, mice lacking MMP-9, a key MMP in tissue remodeling (Stamenkovic, 2003), were also examined and found to experience a much higher increase in tail volume during secondary lymphedema. Thus, this characterization of the mouse tail model and correlation of molecular, cellular, and physiological changes over time lends new insight into the pathophysiology of secondary lymphedema, including the observation that lymphatic hyperplasia and VEGF-C overexpression may be key responses to chronic swelling.

Materials and methods

Mouse tail model of lymphedema

These studies used 6- to 8 week-old female mice, 10 per group, of the following strains: BALB/c (Charles River Laboratories, Wilmington, MA), FVB/NJ (Charles River Laboratories, France), and MMP-9 null on an FVB background (FVB.Cg-Mmp9^{tm1Tv}/J; The Jackson Laboratory, Bar Harbor, ME). Mice were anesthetized with a subcutaneous injection of ketamine (65 mg/kg), xylazine (13 mg/kg), and acepromazine (2 mg/kg). An analgesic, butorphanol (0.05 mg/kg), was administered subcutaneously twice daily for three days following the procedure. All protocols were approved by the ACUC of Northwestern University and the Veterinary Authorities of the Canton Vaud according to Swiss law.

To create lymphedema, a circumferential incision was made through the dermis close to the tail base to sever the dermal lymphatic vessels. The edges of this incision were then pushed apart with a cauterizing iron, thereby disturbing the deeper lymphatics, preventing superficial bleeding, and creating a 2–3 mm gap to delay wound closure. Care was taken to maintain the integrity of the major underlying blood vessels and tendons so that the tail distal to the incision did not become necrotic. An age-matched control group of mice was maintained without this procedure to measure the baseline tail volume during the time course of the analysis.

Daily volume measurements of the tails, from the tip to the distal edge of the wound, were made by volume displacement. For untreated mice, a circumferential mark was made on the tail 10mm from the tail base to mimic the incision site for reproducibility in measuring.

Sample preparation

Mice were sacrificed at various times up to 30 days post-procedure. The tail was excised at the site of the edema procedure and the distal tissue was flash frozen in liquid N₂. Tissue samples

were transversely cryosectioned into 12 and 60 μm -thick sections and stored at -80°C until immunostaining.

Microlymphangiography

Mice were anesthetized as above and the integrity of the lymphatic vasculature of the tail was examined by fluorescence microlymphangiography (Hagendoorn et al., 2004; Swartz et al., 1996, 1999). A fluorescently labeled macromolecule (2000 kDa tetramethylrhodamine-conjugated dextran, 2 mg/ml; Molecular Probes, Carlsbad, CA) was injected intradermally at a constant pressure of 45 cm of water into the tip of the tail. Because of its large size, the tracer was taken up by the lymphatics but was excluded from the blood vasculature. As the fluorescent tracer was transported by the lymphatic vessels, it was clearly visible within dermal lymphatic capillaries, thus providing a clear visualization of lymphatic functionality. The filling of the lymphatic vasculature was monitored for 90 min with a Zeiss Axiovert 200M fluorescence microscope and Zeiss MRm camera set at equal exposure time for each mouse.

Immunohistochemistry and histology

To visualize lymphatic vessels, thin (12 μm) and thick (60 μm) sections were co-stained with a primary antibody to the lymphatic-specific marker LYVE-1 (1:500; rabbit polyclonal; Upstate, Charlottesville, VA). Thin sections were also labeled using anti-mouse antibodies for the macrophage-specific surface marker F4/80 (1:50; rat monoclonal; Serotec, Raleigh, NC) and the Langerhans dendritic cell protein langerin (1:50; goat polyclonal; Santa Cruz Biotechnology, Santa Cruz, CA). These antibodies were detected with Alexafluor 488 or 594-conjugated donkey, rabbit, and goat IgG secondary antibodies (1:200, Molecular Probes), counterstained with DAPI (Vector Labs, Burlingame, CA), and observed and imaged as above. Thick sections were scanned using a Zeiss LSM 510 Meta confocal microscope. PCNA staining was achieved on thin sections with a monoclonal biotinylated mouse anti-PCNA primary antibody (prediluted; Zymed Laboratories, South San Francisco, CA) and detected with Texas Red-conjugated avidin (Vector Labs).

VEGF-C was labeled immunohistochemically on thin sections. Sections were first fixed in 4% PFA, blocked against endogenous biotin and avidin activity (Biotin Blocking System, Dako, Carpinteria, CA), then labeled with anti-mouse VEGF-C (1:50; goat polyclonal; Santa Cruz) and biotinylated secondary antibody (1:500; AffiniPure rabbit; Jackson ImmunoResearch, West Grove, PA). This was then visualized using the ABC-AP kit and Vector Black (Vector Labs). Sections were counterstained with Orange G (Merck KGaA, Darmstadt, Germany), dehydrated, and mounted with Eukitt (Fluka Chemie AG, Buchs, Switzerland). Images were captured with an Olympus AX70 Microscope and DP70 Camera.

Masson's trichrome was used to stain collagen and Oil red O (Sigma-Aldrich, Buchs, Switzerland) to stain lipids on thin sections. Sections were mounted and imaged as above, except Oil red O stained sections were counterstained with hematoxylin and not dehydrated but immediately mounted with Glycergel mounting medium (Dako).

Image analysis

Images of each tail section were first assembled into complete montages in Photoshop (Adobe Systems, San Jose, CA). To quantify LEC hyperplasia, LECs were defined as cells with a blue (DAPI-stained) nucleus surrounded by green LYVE-1 staining, and lymphatic structures were defined as continuous groups of LYVE-1 labeled cells. The numbers of LECs within each structure were counted in three random 12 μm sections from each animal.

To quantify VEGF-C expression, Metamorph 6.3 image analysis software (Molecular Devices Corp., Sunnyvale, CA) was used. Three labeled sections from each time point were analyzed.

In each, the region between the epidermis and underlying tendon was clearly identified with a freehand tool, and the total intensity within this region was integrated.

Statistics

For quantified data, ANOVA followed by two-tailed Student's *t* tests were performed to determine statistical significance between two groups or among different time points. Data are reported as average \pm standard deviations. Tail volumes are presented as a change over normal, LEC counts as total cells, and VEGF-C as normalized to the maximum.

Results

Degree and sustainability of swelling

All three strains of mice tested (BALB/c, FVB/NJ, and MMP-9 null) sustained reproducible edema for a period of at least 30 days. In the wild-type strains examined, FVB/NJ and BALB/c, tail volume measurements consistently peaked at 15 days following the ligation procedure with a volume increase of 55–75% (Fig. 1). Resolution of edema in these mice also consistently occurred to within 20% of control volume by 30 days. Two FVB/NJ mice were kept for 60 days and their increased tail volumes were sustained (both 17% larger than baseline at day 60) in agreement with past work (Slavin et al., 1999). MMP-9 null mice experienced significantly more tissue swelling than wild-type controls both with a higher peak volume change at 15 days of 115% ($P=0.0287$) and higher 30 day volume change of 75%.

Matrix changes and lipid accumulation

In normal tail skin, the dermis possesses a much higher density of collagen than the underlying hypodermis. One day after lymphatic disruption, we observed an immediate reduction in collagen density throughout the dermis, whereas the subcutaneous tissue layer of the hypodermis was drastically swollen (Fig. 2A). Within the first week, however, the density of collagen in the dermis increased, and by day 14 the collagen architecture in the dermis appeared similar to that of normal tissue. The change in tail volume was thus mainly due to hypodermal swelling. The hypodermis remained swollen with decreased collagen density until day 30, when collagen density again appeared normal, although total tissue volume was significantly increased.

In addition to its propensity to accumulate fluid and swell, the hypodermis also exhibited a striking increase in lipid deposition (Fig. 2B). Lipid accumulation in the hypodermis, visualized through Oil red O staining, became visible after 7 days, peaked at 14 days, and was maintained through 30 days. Macrophages were also present throughout the dermis and hypodermis in edematous skin at all time points examined (Fig. 2C).

Lymphatic function in edematous tail skin

The lymphatic network of the mouse tail skin consists of a regular, hexagonal network of dermal lymphatic capillaries that are easily visualized by fluorescence microlymphangiography (Hagendoorn et al., 2004; Pytowski et al., 2005; Swartz et al., 1996). Furthermore, measures of how much volume is infused into the tail at fixed pressure, along with infusion distance, can be used to estimate hydraulic conductivity and lymphatic function (Reddy et al., in press; Swartz et al., 1999). Microlymphangiography in normal vs. edematous tails revealed functional insufficiencies in the lymphatics and increased hydraulic conductivity (Fig. 3). In normal mice, the lymphatic capillaries took up $\sim 8 \mu\text{l}$ in 90 min of fluorescent dextran infused into the tail tip at 45 cm water; whereas in contrast, day 10 edematous tails took up $\sim 30 \mu\text{l}$ of dextran in 90 min at the same pressure. Despite the increase in hydraulic conductivity and dramatic increase in injected fluid flow rate for a given injection

pressure, the lymphatic capillaries in edematous tails remained functional in taking up the injected fluid tracer; however, fluorescent tracer was visible in the interstitial space around the capillary network, suggesting that the lymphatics in edematous skin were leaky and prone to backflow. After 60 days, the edema was reduced and the lymphatic leakiness was decreased but not entirely resolved.

Lymphatic hyperplasia

Lymphatic ligation and subsequent tissue swelling led to marked morphological changes in the dermal lymphatics caused by the proliferation of LECs and subsequent enlargement of the lymphatic vessels. PCNA-positive LECs were seen in hyper-plastic lymphatic vessels at day 10 (Fig. 4A). A reduced number of PCNA-positive cells were seen in lymphatic vessels at 20 days, and none were visible at 30 days. Confocal microscopy of the lymphatic vessels during edema (Fig. 4B) revealed that the morphology of the vessels was altered, with striking hyperplasia during the period when overall swelling was the greatest (7–21 days). The number of LECs counted in each lymphatic structure was significantly higher than in normal vessels, peaking at 7 days ($P < 0.001$). After this, the number of LECs per structure decreased but still remained significantly higher than normal throughout the resolution of edema ($P < 0.001$) (Fig. 4C).

Heightened VEGF-C expression

VEGF-C expression in normal tail skin was low, consistent with earlier findings (Boardman and Swartz, 2003; Goldman et al., 2005; Rutkowski et al., in press). In the first days after lymphatic ligation, tail swelling and lymphatic vessel hyper-plasia were already significant but VEGF-C expression remained low (Fig. 5). VEGF-C began to increase throughout the edematous tissue at day 7 ($P = 0.037$) and peaked at day 14 ($P = 0.022$). Expression remained high as the swelling began to resolve at day 21 ($P = 0.014$) and was decreased to normal levels at day 30. VEGF-C was mostly concentrated in the hypodermis, where the swelling was maximal but few lymphatic vessels were present. Thus, although VEGF-C was upregulated in edematous tissue, its expression patterns did not necessarily correlate with lymphatic hyperplasia.

Dendritic cell migration

Langerhans dendritic cells reside in the epidermis and migrate to the lymphatics in response to immune challenges (Randolph et al., 2005). In normal tissue, Langerin+ cells were seen both in the epidermis and in the dermis near lymphatic vessels (Fig. 6). However, these cells were confined to the epidermis after lymphatic ligation until day 14, where they appeared to be migrating towards the lymphatics despite the hyperplastic appearance and transport insufficiencies of the lymphatic vessels (Fig. 6). Therefore, at days 14, 21, and 30, correlating with the peak and resolution phase of edema, these cells were present in the dermis near the hyperplastic lymphatic vessels.

Increased fluid uptake and propensity for edema in MMP-9 null mice

In untreated (non-edematous) mice, the lymphatic capillary architecture was similar in MMP-9 null vs. wild-type control tails as visualized by microlymphangiography (Figs. 7A and B), although the lymphatic networks in MMP-9 null mice appeared much brighter than in control mice and took up 50% more fluid in 90 min at a fixed infusion pressure of 45 cm water than did the controls (12 vs. 8 μ l). Although there appeared to be minor indications of fluorescent tracer outside of the well-defined lymphatic vessels (Fig. 7B), there was little evidence of actual lymph leakage from the capillaries into the interstitium, as was clearly seen in edematous tails. These minor defects were likely the result of the increased brightness of the tail images resulting from increased tracer uptake (images were taken at the same exposure). Confocal imaging of

the lymphatic vessels revealed no obvious differences in lymphatic vessel morphology from normal mice, suggesting that the increased fluid tracer uptake in untreated MMP-9 null mice was the result of either more efficient lymphatic transport or a higher hydraulic conductivity of extracellular matrix.

Surprisingly, despite the apparently normal or above normal functionality of the lymphatics, MMP-9 null mice with lymphatic ligation exhibited a far greater degree of swelling than did wild-type mice, particularly between 7 and 21 days ($P < 0.001$; Fig. 1), and took longer to resolve ($P < 0.001$; Fig. 1). This swelling was so rapid and so extensive that it actually led to necrosis of the tail in two of the seven mice tested. Examination of the extracellular matrix of the tail skin revealed that the collagen density of MMP-9 null mice was, in fact, less than that of the wild-type controls. This was the case both in untreated tails and those after 14 days of edema (Figs. 7D and E). Therefore, the increased tracer fluid uptake into the tail seen in untreated MMP-9 null mice was probably due to an increase in hydraulic conductivity. This difference in the matrix architecture, in conjunction with the inability to maintain tail volume during swelling, suggests that MMP-9 plays an important role in the maintenance of extracellular tissue fluid.

Discussion

To help elucidate the pathophysiology of secondary lymphedema, we characterized and correlated key molecular-, cellular-, and tissue-level changes over time in the mouse tail edema model and demonstrated its reproducibility and sustainability. We found that in otherwise healthy tissue, sustained swelling induced by lymphatic ligation leads to lymphatic hyperplasia and VEGF-C upregulation. Interestingly, LEC proliferation began before VEGF-C upregulation, suggesting that lymphatic hyperplasia may be supported by VEGF-C only later, from day 14 (the peak in tail volume) through day 30. Also, the maximal VEGF-C expression was seen within the hypodermis, where most of the tail swelling was maintained but where lymphatic vessels were scarcer than in the dermis. This VEGF-C upregulation may therefore be a response to the accumulated fluid in the hypodermis.

Lymphatic vessel hyperplasia in the absence of VEGF-C presents a quandary when examining the potential for VEGF-C delivery as a therapy for lymphedema. Whereas VEGF-C treatment has been shown to hasten the resolution of edema in the mouse tail model, this result was accomplished by hastening lymphangiogenesis across the ligation (Yoon et al., 2003) rather than necessarily inducing a change in the local function of lymphatics. Therefore, delivery may only be beneficial in cases where transport insufficiencies are the result of a lack of lymphatic vessels in the tissue by inducing the growth of new lymphatic capillaries (Karkkainen et al., 2001; Szuba et al., 2002; Yoon et al., 2003). Excess VEGF-C has also been shown to cause hyperplasia of lymphatic vessels when no other lymphatic defects were present (Goldman et al., 2005). Therefore, our results showing that both increased VEGF-C and lymphatic hyperplasia are a response to tissue swelling suggesting that VEGF-C therapy may have limited use for treating secondary lymphedema.

In examining functional lymphatic uptake during lymphedema, we found that the disruption in lymphatic transport led to an increase in fluorescent tracer uptake during microlymphangiography in part from the well-established increase in hydraulic conductivity of the interstitium resulting from the breakdown of the tail matrix (Aarli and Aukland, 1991; Bert and Reed, 1995; Swartz et al., 1999). We also found that the dilated, hyperplastic lymphatics were less effective at lymph transport and leaked lymph back into the interstitium. It is not known whether or how the decreased lymphatic transport function contributed to the increased lipid accumulation in adipocytes.

In addition to decreased fluid drainage from the interstitium, hyperplastic lymphatics may exacerbate the edematous pathology by decreasing immune cell trafficking. When stimulated, Langerhans dendritic cells normally migrate from the epidermis into the lymphatic capillaries to traffic to lymph nodes for antigen presentation. In edematous skin, Langerhans cells were not migrating through the dermis until day 14, even though other inflammatory responses like macrophages and massive matrix proteolysis were present earlier in lymphedema. Lack of migration may be due to the absence of migration-directing interstitial flow which only returns once edema is resolving, although it has yet to be demonstrated that interstitial flow specifically guides dendritic cells towards the lymphatics (Randolph et al., 2005). This apparent lack of DC migration to lymphatics during tissue swelling may lead to decreased immune response, which in turn may exacerbate the pathological state of the limb. This notion is consistent with previous work showing that the immune response is compromised in edematous limbs (Olszewski et al., 1990), leaving the tissue more prone to infection and further inflammation.

MMP-9, a key MMP in matrix remodeling (Stamenkovic, 2003), appeared to play an important role in edema prevention. First, the collagen density in the dermis of MMP-9 null mice was lower than that in wild-type mice, both in normal and edematous states. This reduced matrix density may leave the tissue more susceptible to fluid accumulation and tissue swelling. Indeed, MMP-9 null mice were unable to sufficiently counteract the swelling through responsive remodeling of the matrix. Thus, the skin of the mouse tail apparently relies on MMP-9 in remodeling the extracellular matrix to counteract the change in volume.

The reproducibility and sustainability of the mouse tail model of lymphedema were demonstrated across two normal strains and for roughly 20–30 days, respectively, although in some mice (for unknown reasons) edema can be sustained indefinitely (Slavin et al., 1999). This time frame is sufficient to observe key features of chronic edema, including collagen breakdown and remodeling, lymphatic hyperplasia, and abnormal lipid accumulation in the skin, consistent with pathological features observed in longer studies in other models (Kanter et al., 1990; Olszewski, 1973; Szuba et al., 2002). Responsive changes in the dermal matrix during swelling – initial degradation followed by compensatory rebuilding – were also temporally correlated to lipid accumulation and macrophage infiltration throughout the tissue, both chronic indicators of lymphedema (Piller, 1990; Schirger et al., 1962).

In summary, the mouse tail model of lymphedema is reproducible, reliable, and shows many characteristics of chronic secondary lymphedema. We found that sustained tissue swelling due to lymphatic blockage led to marked lymphatic hyperplasia and lipid accumulation, followed by substantial VEGF-C overexpression in the hypodermis. The hyperplastic lymphatic vessels were poorly functional at draining interstitial fluid, and the resulting fluid stagnation may have contributed to decreased Langerhans dendritic cell homing to the lymphatics. These correlations between factors regulating tissue homeostasis and those regulating lymphatic biology during tissue swelling following lymphatic ligation raise important questions in considering treatment strategies aimed at lymphatic growth for alleviating secondary lymphedema.

Acknowledgements

The authors are grateful to Dr. Hugo Schmoekel and Veronique Garea for invaluable assistance with the animals, Miriella Pasquier for sectioning, and Sai T. Reddy and Gabriela Miyazawa for helpful assistance. The authors thank the NIH (RO1-HL075217-01), NSF (BES-0134551), and The Swiss National Science Foundation for funding.

References

Aarli V, Aukland K. Oedema-preventing mechanisms in a low-compliant tissue: studies on the rat tail. *Acta Physiol Scand* 1991;141:489–495. [PubMed: 1877349]

- Bert JL, Reed RK. Flow conductivity of rat dermis is determined by hydration. *Biorheology* 1995;32:17–27. [PubMed: 7548858]
- Boardman KC, Swartz MA. Interstitial flow as a guide for lymphangiogenesis. *Circ Res* 2003;92:801–808. [PubMed: 12623882]
- Brice G, Mansour S, Bell R, Collin JR, Child AH, Brady AF, Sarfarazi M, Burnand KG, Jeffery S, Mortimer P, Murday VA. Analysis of the phenotypic abnormalities in lymphoedema-distichiasis syndrome in 74 patients with FOXC2 mutations or linkage to 16q24. *J Med Genet* 2002;39:478–483. [PubMed: 12114478]
- Dagenais SL, Hartsough RL, Erickson RP, Witte MH, Butler MG, Glover TW. Foxc2 is expressed in developing lymphatic vessels and other tissues associated with lymphedema-distichiasis syndrome. *Gene Expression Patterns* 2004;4:611–619. [PubMed: 15465483]
- Daroczy J. Pathology of lymphedema. *Clin Dermatol* 1995;13:433–444. [PubMed: 8665454]
- Foldi E. The treatment of lymphedema. *Cancer* 1998;83:2833–2834. [PubMed: 9874407]
- Gale NW, Thurston G, Hackett SF, Renard R, Wang Q, McClain J, Martin C, Witte C, Witte MH, Jackson D, et al. Angiopoietin-2 is required for postnatal angiogenesis and lymphatic patterning, and only the latter role is rescued by Angiopoietin-1. *Dev Cell* 2002;3:411–423. [PubMed: 12361603]
- Goldman J, Le TX, Skobe M, Swartz MA. Overexpression of VEGF-C causes transient lymphatic hyperplasia but not increased lymphangiogenesis in regenerating skin. *Circ Res* 2005;96:1193–1199. [PubMed: 15890974]
- Hagendoorn J, Padera TP, Kashiwagi S, Isaka N, Noda F, Lin MI, Huang PL, Sessa WC, Fukumura D, Jain RK. Endothelial nitric oxide synthase regulates microlymphatic flow via collecting lymphatics. *Circ Res* 2004;95:204–209. [PubMed: 15192027]
- Han LY, Chang TS, Hwang WY. Experimental model of chronic limb lymphedema and determination of lymphatic and venous pressures in normal and lymphedematous limbs. *Ann Plast Surg* 1985;15:303–312. [PubMed: 4083729]
- Harvey NL, Srinivasan RS, Dillard ME, Johnson NC, Witte MH, Boyd K, Sleeman MW, Oliver G. Lymphatic vascular defects promoted by Prox1 haploinsufficiency cause adult-onset obesity. *Nat Genet* 2005;37:1072–1081. [PubMed: 16170315]
- Jeltsch M, Kaipainen A, Joukov V, Meng X, Lakso M, Rauvala H, Swartz M, Fukumura D, Jain RK, Alitalo K. Hyperplasia of lymphatic vessels in VEGF-C transgenic mice. *Science* 1997;276:1423–1425. [PubMed: 9162011]
- Kanter MA, Slavin SA, Kaplan W. An experimental model for chronic lymphedema. *Plast Reconstr Surg* 1990;85:573–580. [PubMed: 2315397]
- Karkkainen MJ, Saaristo A, Jussila L, Karila KA, Lawrence EC, Pajusola K, Bueler H, Eichmann A, Kauppinen R, Kettunen MI, et al. A model for gene therapy of human hereditary lymphedema. *Proc Natl Acad Sci U S A* 2001;98:12677–12682. [PubMed: 11592985]
- Kriederman BM, Myloyde TL, Witte MH, Dagenais SL, Witte CL, Rennels M, Bernas MJ, Lynch MT, Erickson RP, Caulder MS, et al. FOXC2 haploinsufficient mice are a model for human autosomal dominant lymphedema-distichiasis syndrome. *Hum Mol Genet* 2003;12:1179–1185. [PubMed: 12719382]
- Kukk E, Lymboussaki A, Taira S, Kaipainen A, Jeltsch M, Joukov V, Alitalo K. VEGF-C receptor binding and pattern of expression with VEGFR-3 suggests a role in lymphatic vascular development. *Development* 1996;122:3829–3837. [PubMed: 9012504]
- Mortimer PS. Therapy approaches for lymphedema. *Angiology* 1997;48:87–91. [PubMed: 8995349]
- Oh SJ, Jeltsch MM, Birkenhager R, McCarthy JE, Weich HA, Christ B, Alitalo K, Wilting J. VEGF and VEGF-C: specific induction of angiogenesis and lymphangiogenesis in the differentiated avian chorioal-lantoic membrane. *Dev Biol* 1997;188:96–109. [PubMed: 9245515]
- Oliver G, Alitalo K. The lymphatic vasculature: recent progress and paradigms. *Annu Rev Cell Dev Biol* 2005;21:457–483. [PubMed: 16212503]
- Olszewski W. On the pathomechanism of development of postsurgical lymphedema. *Lymphology* 1973;6:35–51. [PubMed: 4691971]
- Olszewski WL, Engeset A, Romaniuk A, Grzelak I, Ziolkowska A. Immune cells in peripheral lymph and skin of patients with obstructive lymphedema. *Lymphology* 1990;23:23–33. [PubMed: 2352440]

- Petrova TV, Karpanen T, Norrmen C, Mellor R, Tamakoshi T, Finegold D, Ferrell R, Kerjaschki D, Mortimer P, Yla-Herttuala S, et al. Defective valves and abnormal mural cell recruitment underlie lymphatic vascular failure in lymphedema distichiasis. *Nat Med* 2004;10:974–981. [PubMed: 15322537]
- Piller NB. Macrophage and tissue changes in the developmental phases of secondary lymphoedema and during conservative therapy with benzopyrone. *Arch Histol Cytol* 1990;53:209–218. [PubMed: 2252630](Suppl)
- Pytowski B, Goldman J, Persaud K, Wu Y, Witte L, Hicklin DJ, Skobe M, Boardman KC, Swartz MA. Complete and specific inhibition of adult lymphatic regeneration by a novel VEGFR-3 neutralizing antibody. *J Natl Cancer Inst* 2005;97:14–21. [PubMed: 15632376]
- Randolph GJ, Angeli V, Swartz MA. Dendritic-cell trafficking to lymph nodes through lymphatic vessels. *Nat Rev Immunol* 2005;5:617–628. [PubMed: 16056255]
- Reddy ST, Berk DA, Jain RK, Swartz MA. A sensitive in vivo model for quantifying interstitial convective transport of injected macromolecules and monoparticles. *J Appl Physiol*. 10.1152/jappphysiol.00389.2006in press
- Rockson SG. Lymphedema. *Am J Med* 2001;110:288–295. [PubMed: 11239847]
- Rutkowski JM, Boardman KC, Swartz MA. Characterization of lymphangiogenesis in a model of adult skin regeneration. *Am J Physiol, Heart Circ Physiol*. 10.1152/ajpheart.00038.2006in press
- Schirger A, Harrison EG Jr, Janes JM. Idiopathic lymphedema. Review of 131 cases. *JAMA* 1962;182:14–22. [PubMed: 14498461]
- Slavin SA, Van den Abbeele AD, Losken A, Swartz MA, Jain RK. Return of lymphatic function after flap transfer for acute lymphedema. *Ann Surg* 1999;229:421–427. [PubMed: 10077056]
- Stamenkovic I. Extracellular matrix remodelling: the role of matrix metalloproteinases. *J Pathol* 2003;200:448–464. [PubMed: 12845612]
- Swartz MA, Berk DA, Jain RK. Transport in lymphatic capillaries: I. Macroscopic measurements using residence time distribution theory. *Am J Physiol* 1996;270:H324–H329. [PubMed: 8769768]
- Swartz MA, Kaipainen A, Netti PA, Brekken C, Boucher Y, Grodzinsky AJ, Jain RK. Mechanics of interstitial-lymphatic fluid transport: theoretical foundation and experimental validation. *J Biomech* 1999;32:1297–1307. [PubMed: 10569708]
- Szuba A, Skobe M, Karkkainen MJ, Shin WS, Beynet DP, Rockson NB, Dakhil N, Spilman S, Goris ML, Strauss HW. Therapeutic lymphangiogenesis with human recombinant VEGF-C. *FASEB J* 2002;16:1985–1987. [PubMed: 12397087]
- Wang GY, Zhong SZ. A model of experimental lymphedema in rats' limbs. *Microsurgery* 1985;6:204–210. [PubMed: 4088029]
- Wigle JT, Oliver G. Prox1 function is required for the development of the murine lymphatic system. *Cell* 1999;98:769–778. [PubMed: 10499794]
- Witte MH, Bernas MJ, Martin CP, Witte CL. Lymphangiogenesis and lymphangiodyplasia: from molecular to clinical lymphology. *Microsc Res Tech* 2001;55:122–145. [PubMed: 11596157]
- Yoon YS, Murayama T, Gravereaux E, Tkebuchava T, Silver M, Curry C, Wecker A, Kirchmair R, Hu CS, Kearney M, et al. VEGF-C gene therapy augments postnatal lymphangiogenesis and ameliorates secondary lymphedema. *J Clin Invest* 2003;111:717–725. [PubMed: 12618526]

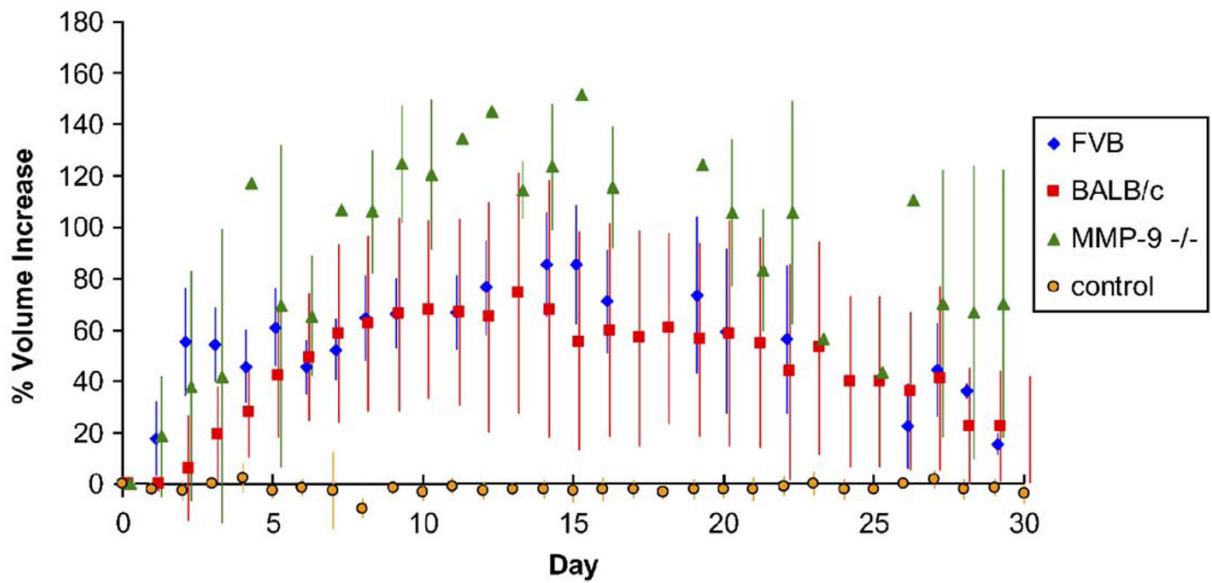


Fig. 1.

Tail volume changes following lymphatic ligation. Two control strains of mice, FVB/NJ (blue diamonds) and BALB/c (red squares), displayed nearly equivalent swelling and resolution patterns, and both peaked at 15 days. Transgenic mice lacking MMP-9 (green triangles) also displayed maximum volume increase at 15 days but showed a significantly greater extent of swelling compared to the wild-type strains as well as a longer resolution time. (For interpretation of the references to colour in this figure legend, the reader is referred to the web version of this article.)

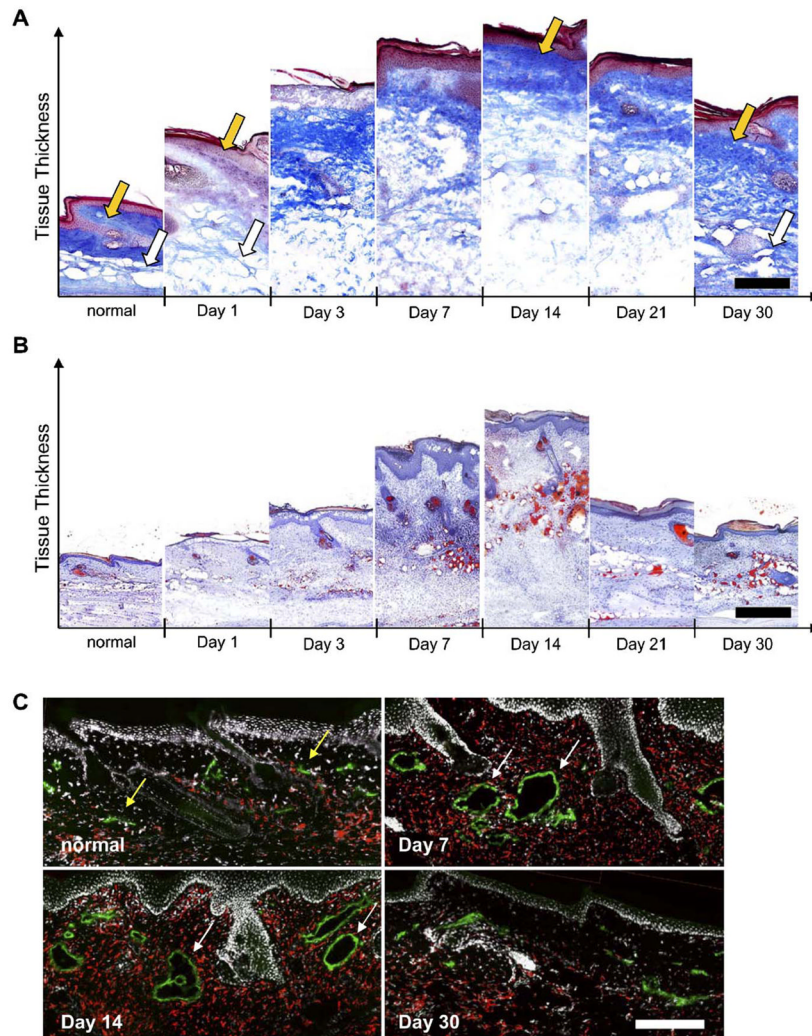


Fig. 2. Extracellular matrix density, lipid accumulation, and macrophage presence in edematous tails. (A) In normal skin, a collagen-dense dermis (gold arrow) and less dense hypodermis (white arrow) was seen. One day following lymphatic ligation, the collagen network was degraded in both the dermis and hypodermis as fluid accumulated. At day 14 when tail volume reaches its peak, the collagen density (blue) in the dermis returned to normal (gold arrow) whereas the architecture of the hypodermis remains severely compromised. At day 30, the collagen architecture throughout the tissue appeared normal. (B) Oil red O staining showed that the hypodermis dramatically filled with lipids (red) at day 7 and that this accumulation was maintained through 30 days. (C) Macrophages (red) were also present in high numbers at all times during edema. Note the hyperplastic lymphatic (green) vessels at days 7 and 14 (marked by white arrows) as compared to normal vessels (gold arrows). Scale bars=200 μ m. (For interpretation of the references to colour in this figure legend, the reader is referred to the web version of this article.)

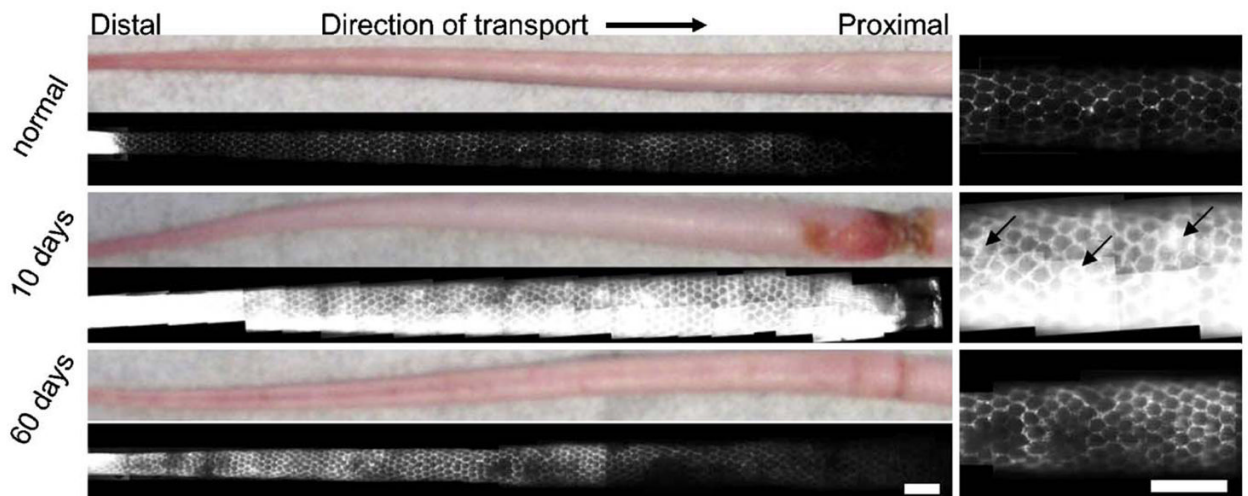


Fig. 3.

Fluorescence microlymphangiography revealed leaky lymphatic capillaries in edematous skin, with higher magnification images shown at right. The normal mouse tail skin possessed a well-defined hexagonal network of dermal lymphatics that transport the fluorescent tracer proximally (left to right) from infusion into the tip of the tail. At 10 days of lymphedema, the tail was swollen and the fluorescent tracer filled both the lymphatic vessels and the interstitial space (back flow indicated by arrows). At 60 days, lymphatic transport was improved but not fully restored. All images were taken with the same exposure time. Scale bars=2 mm.

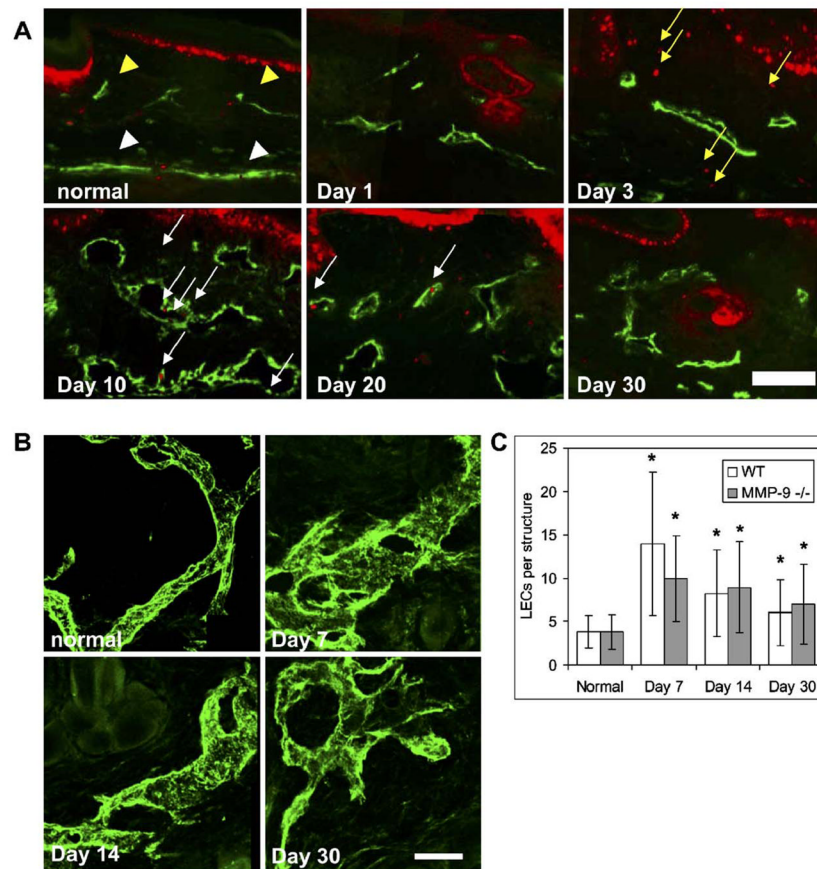


Fig. 4. Lymphatic morphology changes during edema. (A) Normal tissue showed few proliferating cells and small superficial lymphatics (gold arrowheads) with the underlying collecting lymphatic vessels (white arrowheads). PCNA staining (red) indicated that as the tail volume increased, lymphatic endothelial cells (LECs, green) proliferated (white arrows). At day 10, LECs in the vessels were proliferating and the vessels were hyperplastic. This LEC proliferation was reduced at 20 days and absent at 30 days. Edema also induced the proliferation of other cells in the dermis (gold arrows). (B) Confocal microscopy of the dermal lymphatic vessels demonstrated the drastic hyperplasia and morphological changes associated with edema at 7 and 14 days, with an abnormal morphology still present at 30 days. Scale bars=100 μ m. (C) The number of LECs per lymphatic structure was greatest at day 7 in both wild-type and MMP-9 deficient mice ($*P<0.05$ over control). (For interpretation of the references to colour in this figure legend, the reader is referred to the web version of this article.)

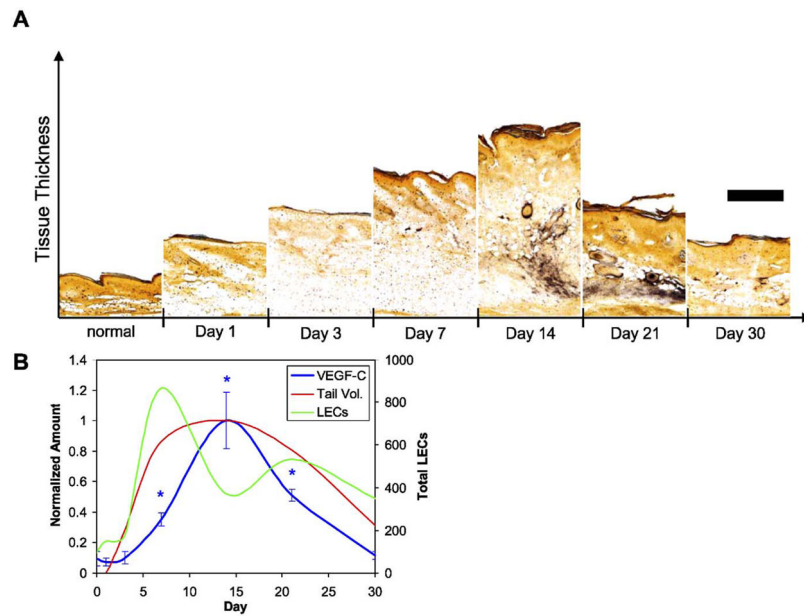


Fig. 5. VEGF-C expression in edematous tails. (A) VEGF-C expression (black) was normally quite low and remained so during the onset of edema (through 7 days); orange indicated collagen by orange G staining. At 14 days, however, VEGF-C was greatly increased and remained high at day 21. Scale bar=200 μ m. (B) The peak of VEGF-C expression (integrated intensity) lagged behind the peak of LEC proliferation and vessel hyperplasia ($*P < 0.05$ vs. control). (For interpretation of the references to colour in this figure legend, the reader is referred to the web version of this article.)

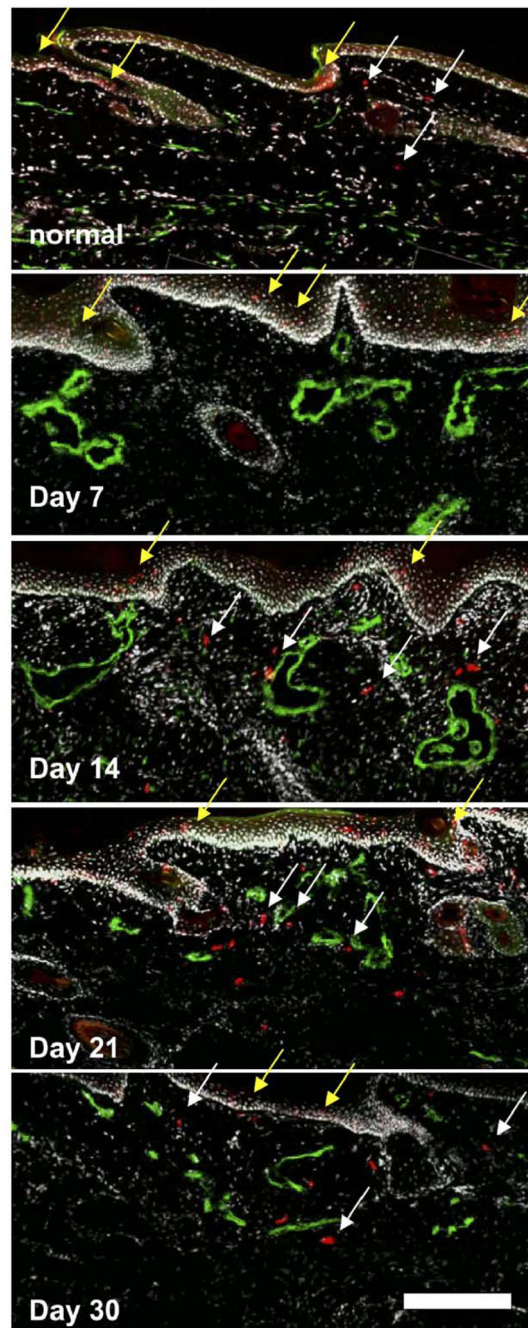


Fig. 6. Langerhans dendritic cell (DC) trafficking during edema. In normal skin, some DCs (red) were seen between the epidermis and lymphatic vessels (green) in the skin, indicating normal migration. After 7 days of edema, no DCs were found below the epidermis. At 14, 21, and 30 days, DCs were present in high numbers in the dermis and near the hyperplastic lymphatic vessels, indicating migration. Yellow arrows indicate some DCs in the epidermis, and white arrows indicate migrating DCs. Scale bar=200 μ m. (For interpretation of the references to colour in this figure legend, the reader is referred to the web version of this article.)

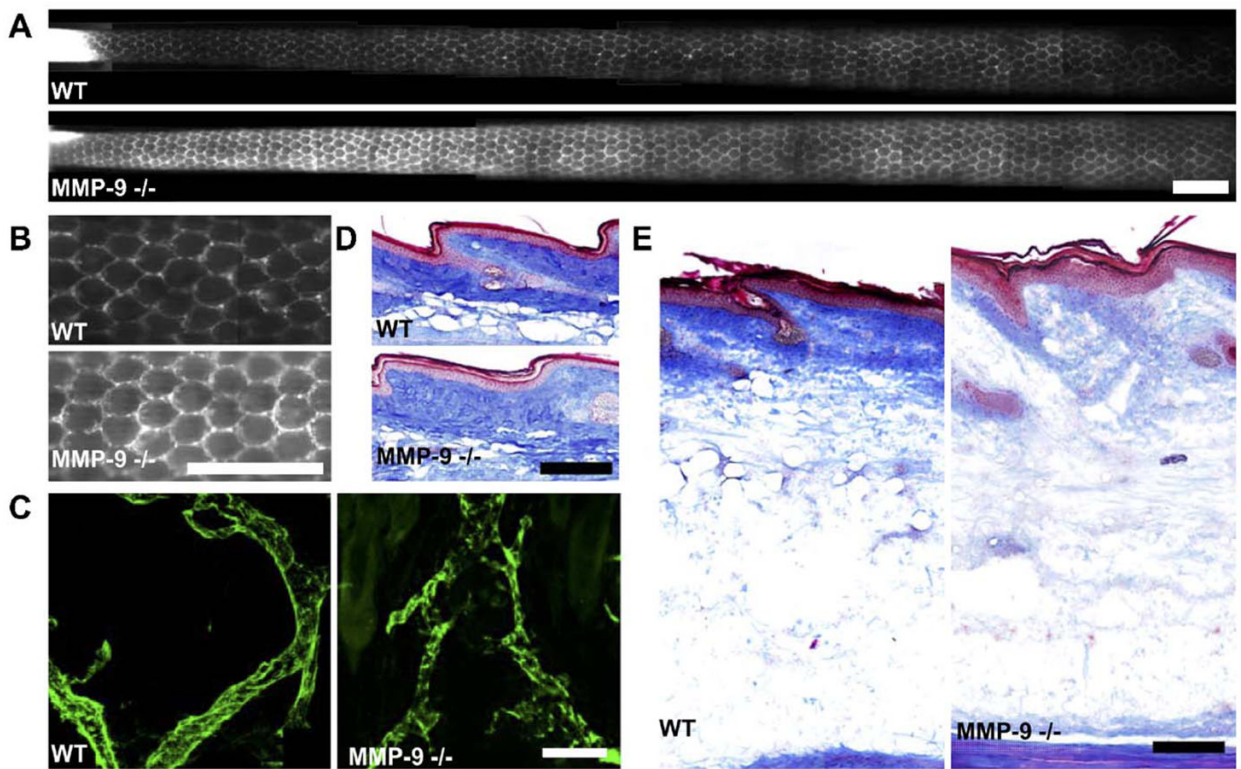


Fig. 7. Differences in lymphatic function and morphology and extracellular matrix architecture in MMP-9 null mice vs. wild-type controls. (A) In untreated animals, constant-pressure infusion of fluorescent tracer led to 50% more uptake by MMP-9 null mice vs. wild-type controls. The lymphatic vessel networks of the MMP-9 null mice appeared to be much brighter (with equal exposure time) than those of the wild-type controls, indicating a higher uptake rate. Scale bar=2 mm. (B) Higher magnification images of the lymphatic structures showed normally functioning vessels with no backflow; scale bar=2 mm. (C) Confocal images of the lymphatic vessels (green) in each type of mouse showed little or no morphological differences between wild-type and MMP-9 null mice; scale bar=100 μ m. (D) In untreated animals, the collagen matrix (blue) appeared to be less dense in the dermis of the MMP-9 null mice than in that of the FVB/NJ mice; scale bar=200 μ m. (E) After 14 days of edema, the dermal collagen density appeared normal in the wild-type control mice but remained largely degraded in the MMP-9 null mice; scale bar=200 μ m. (For interpretation of the references to colour in this figure legend, the reader is referred to the web version of this article.)